Constraints on Heavy Decaying Dark Matter from 570 Days of LHAASO Observations

Cao, Z.; LHAASO Collaboration; Ando, S.; Chianese, M.; Miele, G.; Ng, K.C.Y.

DOI
10.1103/PhysRevLett.129.261103

Publication date
2022

Document Version
Final published version

Published in
Physical Review Letters

Editors' Suggestion Featured in Physics

Constraints on Heavy Decaying Dark Matter from 570 Days of LHAASO Observations

Zhen Cao,[1,2,3] F. Aharonian,[4,5] Q. An,[6,7] Axikegu,[8] L. X. Bai,[9] Y. X. Bai,[1,3] Y. W. Bao,[10] D. Bastieri,[11] X. J. Bi,[1,2,3] Y. J. Bi,[1,3] J. T. Cai,[11] Zhe Cao,[6,7] J. Chang,[12] J. F. Chang,[1,3,6] E. S. Chen,[1,2,3] Liang Chen,[1,2,3] Liang Chen,[13] Long Chen,[8] M. J. Chen,[1,3] M. L. Chen,[1,3,6] Q. H. Chen,[8] S. H. Chen,[1,2,3] S. Z. Chen,[1,3,§] T. L. Chen,[14] Y. Chen,[10] H. L. Cheng,[2,15,14] N. Cheng,[1,3] Y. D. Cheng,[1,3] S. W. Cui,[16] X. H. Cui,[15] Y. D. Cui,[17] B. D'Ettorre Piazzoli,[18] B. Z. Dai,[19] H. L. Dai,[1,3,6] Z. G. Dai,[7] Danzengluobu,[14] D. della Volpe,[20] K. K. Duan,[12] J. H. Fan,[11] Y. Z. Fan,[12] Z. X. Fan,[1,3] J. Fang,[19] K. Fang,[1,3] C. F. Feng,[21] L. Feng,[12] S. H. Feng,[1,3] X. T. Feng,[21] Y. L. Feng,[14] B. Gao,[1,3] C. D. Gao,[21] L. Q. Gao,[1,2,3] Q. Gao,[14] W. Gao,[1,3] W. K. Gao,[1,2,3] M. M. Ge,[19] L. S. Geng,[1,3] G. H. Gong,[22] Q. B. Gou,[1,3] M. H. Gu,[1,3,6] F. L. Guo,[13] J. G. Guo,[1,2,3] X. L. Guo,[8] Y. Q. Guo,[1,3] Y. Y. Guo,[12] Y. A. Han,[23] H. H. He,[1,2,3] H. N. He,[12] S. L. He,[11] X. B. He,[17] Y. He,[8] M. Heller,[20] Y. K. Hor,[17] C. Hou,[1,3] X. Hou,[24] H. B. Hu,[1,2,3] Q. Hu,[7,12] S. Hu,[9] S. C. Hu,[1,2,3] X. J. Hu,[22] D. H. Huang,[8] W. H. Huang,[21] X. T. Huang,[21] X. Y. Huang,[12] Y. Huang,[1,2,3] Z. C. Huang,[8] X. L. Ji,[1,3,6] H. Y. Jia,[8] K. Jia,[21] K. Jiang,[6,7] Z. J. Jiang,[19] M. Jin,[1,3] M. M. Kang,[9] T. Ke,[1,3] D. Kuleshov,[25] K. Levochkin,[25] B. B. Li,[16] Cheng Li,[6,7] Cong Li,[1,3] F. Li,[1,3,6] H. B. Li,[1,3] H. C. Li,[1,3] H. Y. Li,[7,12] J. Li,[7,12] Jian Li,[7] Jie Li,[1,3,6] K. Li,[1,3] W. L. Li,[21] X. R. Li,[1,3] Xin Li,[6,7] Xin Li,[8] Y. Z. Li,[1,2,3] Zhe Li,[1,3,*] Zhuo Li,[26] E. W. Liang,[27] Y. F. Liang,[27] S. J. Lin,[17] B. Liu,[7] C. Liu,[1,3] D. Liu,[21] H. Liu,[8] H. D. Liu,[23] J. Liu,[1,3] J. L. Liu,[28] J. S. Liu,[17] J. Y. Liu,[1,3] M. Y. Liu,[14] R. Y. Liu,[10] S. M. Liu,[8] W. Liu,[1,3] Y. Liu,[11] Y. N. Liu,[22] W. J. Long,[8] R. Lu,[19] Q. Luo,[16] H. K. Lv,[1,3] B. Q. Ma,[26] L. L. Ma,[1,3] X. H. Ma,[1,3] J. R. Mao,[24] A. Masood,[8] Z. Min,[1,3] W. Mitthumsiri,[29] Y. C. Nan,[21] Z. W. Ou,[17] B. Y. Pang,[8] P. Pattarakijwanich,[29] Z. Y. Pei,[11] M. Y. Qi,[1,3] Y. Q. Qi,[16] B. Q. Qiao,[1,3] J. J. Qin,[7] D. Ruffolo,[29] A. Sáiz,[29] C. Y. Shao,[17] L. Shao,[16] O. Shchegolev,[25,30] X. D. Sheng,[1,3] J. Y. Shi,[1,3] H. C. Song,[26] Yu. V. Stenkin,[25,30] V. Stepanov,[25] Y. Su,[12] Q. N. Sun,[8] X. N. Sun,[27] Z. B. Sun,[31] P. H. T. Tam,[17] Z. B. Tang,[6,7] W. W. Tian,[2,15] B. D. Wang,[1,3] C. Wang,[31] H. Wang,[8] H. G. Wang,[11] J. C. Wang,[24] J. S. Wang,[28] L. P. Wang,[21] L. Y. Wang,[1,3] R. Wang,[21] R. N. Wang,[8] W. Wang,[17] X. G. Wang,[27] X. Y. Wang,[10] Y. Wang,[8] Y. D. Wang,[1,3] Y. J. Wang,[1,3] Y. P. Wang,[1,2,3] Z. H. Wang,[9] Z. X. Wang,[19] Zhen Wang,[28] Zheng Wang,[1,3,6] D. M. Wei,[12] J. J. Wei,[12] Y. J. Wei,[1,2,3] T. Wen,[19] C. Y. Wu,[1,3] H. R. Wu,[1,3] S. Wu,[1,3] X. F. Wu,[12] Y. S. Wu,[7] S. Q. Xi,[1,3] J. Xia,[7,12] J. J. Xia,[8] G. M. Xiang,[2,13] D. X. Xiao,[14] G. Xiao,[1,3] G. G. Xin,[1,3] Y. L. Xin,[8] Y. Xing,[13] Z. Xiong,[1,2,3] D. L. Xu,[28] R. X. Xu,[26] L. Xue,[21] D. H. Yan,[24] J. Z. Yan,[12] C. W. Yang,[9] F. F. Yang,[1,3,6] H. W. Yang,[17] J. Y. Yang,[17] L. L. Yang,[17] M. J. Yang,[1,3] R. Z. Yang,[7] S. B. Yang,[19] Y. H. Yao,[9] Z. G. Yao,[1,3] Y. M. Ye,[22] L. Q. Yin,[1,3] N. Yin,[21] X. H. You,[1,3] Z. Y. You,[1,2,3] Y. H. Yu,[7] Q. Yuan,[12] H. Yue,[1,2,3] H. D. Zeng,[12] T. X. Zeng,[1,3,6] W. Zeng,[19] Z. K. Zeng,[1,2,3] M. Zha,[1,3] X. X. Zhai,[1,3] B. B. Zhang,[10] F. Zhang,[8] H. M. Zhang,[10] H. Y. Zhang,[1,3] J. L. Zhang,[15] L. X. Zhang,[11] Li Zhang,[19] Lu Zhang,[16] P. F. Zhang,[19] P. P. Zhang,[7,12] R. Zhang,[7,12] S. B. Zhang,[2,15] S. R. Zhang,[16] S. S. Zhang,[1,3] X. Zhang,[10] X. P. Zhang,[1,3] Y. F. Zhang,[8] Y. L. Zhang,[1,3] Yi Zhang,[1,12] Yong Zhang,[1,3] B. Zhao,[8] J. Zhao,[1,3] L. Zhao,[6,7] L. Z. Zhao,[16] S. P. Zhao,[12,21] F. Zheng,[31] Y. Zheng,[8] B. Zhou,[1,3] H. Zhou,[28] J. N. Zhou,[13] P. Zhou,[10] R. Zhou,[9] X. X. Zhou,[8] C. G. Zhu,[21] F. R. Zhu,[8] H. Zhu,[15] K. J. Zhu,[1–3,6] X. Zuo,[1,3]

(LHAASO Collaboration)[32,33]

S. Ando,[32,33] M. Chianese,[34,35,†] D. F. G. Fiorillo,[34,35,36] G. Miele,[34,35,37] and K. C. Y. Ng[38,‡]

[1]*Key Laboratory of Particle Astrophyics and Experimental Physics Division and Computing Center, Institute of High Energy Physics, Chinese Academy of Sciences, 100049 Beijing, China*
[2]*University of Chinese Academy of Sciences, 100049 Beijing, China*
[3]*TIANFU Cosmic Ray Research Center, Chengdu, Sichuan, China*
[4]*Dublin Institute for Advanced Studies, 31 Fitzwilliam Place, 2 Dublin, Ireland*
[5]*Max-Planck-Institut for Nuclear Physics, P.O. Box 103980, 69029 Heidelberg, Germany*
[6]*State Key Laboratory of Particle Detection and Electronics, China*
[7]*University of Science and Technology of China, 230026 Hefei, Anhui, China*
[8]*School of Physical Science and Technology and School of Information Science and Technology, Southwest Jiaotong University, 610031 Chengdu, Sichuan, China*
[9]*College of Physics, Sichuan University, 610065 Chengdu, Sichuan, China*
[10]*School of Astronomy and Space Science, Nanjing University, 210023 Nanjing, Jiangsu, China*
[11]*Center for Astrophysics, Guangzhou University, 510006 Guangzhou, Guangdong, China*
[12]*Key Laboratory of Dark Matter and Space Astronomy, Purple Mountain Observatory, Chinese Academy of Sciences, 210023 Nanjing, Jiangsu, China*

[13]*Key Laboratory for Research in Galaxies and Cosmology, Shanghai Astronomical Observatory, Chinese Academy of Sciences, 200030 Shanghai, China*
[14]*Key Laboratory of Cosmic Rays (Tibet University), Ministry of Education, 850000 Lhasa, Tibet, China*
[15]*National Astronomical Observatories, Chinese Academy of Sciences, 100101 Beijing, China*
[16]*Hebei Normal University, 050024 Shijiazhuang, Hebei, China*
[17]*School of Physics and Astronomy (Zhuhai) and School of Physics (Guangzhou) and Sino-French Institute of Nuclear Engineering and Technology (Zhuhai), Sun Yat-sen University, 519000 Zhuhai & 510275 Guangzhou, Guangdong, China*
[18]*Dipartimento di Fisica dell'Università di Napoli "Federico II," Complesso Universitario di Monte Sant'Angelo, via Cinthia, 80126 Napoli, Italy*
[19]*School of Physics and Astronomy, Yunnan University, 650091 Kunming, Yunnan, China*
[20]*Département de Physique Nucléaire et Corpusculaire, Faculté de Sciences, Université de Genève, 24 Quai Ernest Ansermet, 1211 Geneva, Switzerland*
[21]*Institute of Frontier and Interdisciplinary Science, Shandong University, 266237 Qingdao, Shandong, China*
[22]*Department of Engineering Physics, Tsinghua University, 100084 Beijing, China*
[23]*School of Physics and Microelectronics, Zhengzhou University, 450001 Zhengzhou, Henan, China*
[24]*Yunnan Observatories, Chinese Academy of Sciences, 650216 Kunming, Yunnan, China*
[25]*Institute for Nuclear Research of Russian Academy of Sciences, 117312 Moscow, Russia*
[26]*School of Physics, Peking University, 100871 Beijing, China*
[27]*School of Physical Science and Technology, Guangxi University, 530004 Nanning, Guangxi, China*
[28]*Tsung-Dao Lee Institute & School of Physics and Astronomy, Shanghai Jiao Tong University, 200240 Shanghai, China*
[29]*Department of Physics, Faculty of Science, Mahidol University, Bangkok 10400, Thailand*
[30]*Moscow Institute of Physics and Technology, 141700 Moscow, Russia*
[31]*National Space Science Center, Chinese Academy of Sciences, 100190 Beijing, China*
[32]*GRAPPA Institute, University of Amsterdam, 1098 XH Amsterdam, The Netherlands*
[33]*Kavli Institute for the Physics and Mathematics of the Universe (KavliIPMU,WPI), University of Tokyo, Kashiwa, Chiba 277-8583, Japan*
[34]*Dipartimento di Fisica "Ettore Pancini," Università degli studi di Napoli "Federico II", Complesso Univ. Monte S. Angelo, I-80126 Napoli, Italy*
[35]*INFN - Sezione di Napoli, Complesso Univ. Monte S. Angelo, I-80126 Napoli, Italy*
[36]*Niels Bohr International Academy, Niels Bohr Institute, University of Copenhagen, Copenhagen, Denmark*
[37]*Scuola Superiore Meridionale, Università degli studi di Napoli "Federico II", Largo San Marcellino 10, 80138 Napoli, Italy*
[38]*Department of Physics, The Chinese University of Hong Kong, Shatin, New Territories, Hong Kong, China*

(Received 29 March 2022; revised 19 August 2022; accepted 27 October 2022; published 21 December 2022)

The kilometer square array (KM2A) of the large high altitude air shower observatory (LHAASO) aims at surveying the northern γ-ray sky at energies above 10 TeV with unprecedented sensitivity. γ-ray observations have long been one of the most powerful tools for dark matter searches, as, e.g., high-energy γ rays could be produced by the decays of heavy dark matter particles. In this Letter, we present the first dark matter analysis with LHAASO-KM2A, using the first 340 days of data from 1/2-KM2A and 230 days of data from 3/4-KM2A. Several regions of interest are used to search for a signal and account for the residual cosmic-ray background after γ/hadron separation. We find no excess of dark matter signals, and thus place some of the strongest γ-ray constraints on the lifetime of heavy dark matter particles with mass between 10^5 and 10^9 GeV. Our results with LHAASO are robust, and have important implications for dark matter interpretations of the diffuse astrophysical high-energy neutrino emission.

DOI: 10.1103/PhysRevLett.129.261103

Introduction.—Dark matter (DM) is one of the cornerstones of fundamental physics and cosmology, as it accounts for most of the mass of the Universe. So far, DM has evaded all the attempts to detect its nongravitational interactions [1–3]; the identification of its nature is one of the primary goals in modern science [4,5]. In this context, DM indirect-detection searches represent a powerful tool that leverages astrophysical data to probe a variety of DM candidates. Among all the astrophysical messengers, high-energy γ rays have long been an important avenue for achieving some of the best sensitivities in DM searches [6–12]. In this regard, very-high-energy (VHE) γ rays offer a unique possibility to probe heavy DM particles with masses above 100 TeV.

In recent years, VHE γ rays have been detected from several Galactic sources [13–17] as well as from the whole Galactic plane [18]. Away from the Galactic plane, upper limits have been placed on the isotropic diffuse γ-ray flux above 100 TeV [19–21]. While the γ-ray emission from extragalactic sources is significantly suppressed due to the cosmic γ-ray absorption, detectable high-latitude VHE γ rays could be produced through the decays of heavy DM particles in the Galactic halo, as DM annihilations are theoretically disfavored by the unitarity bound in the VHE regime [22]. Decaying heavy DM has been theorized in several models, including WIMPIzillas [23–25], glueballs [26–29], gravitinos [30–32], frozen-in DM [33–36], and other proposals [37–46]. Interestingly, it has also been proposed [47–49] as a source of the diffuse TeV-PeV neutrino flux observed by IceCube [50–52]. Such a scenario has been long studied with multimessenger observations [53–78]. Nevertheless, DM contributions to the diffuse high-energy neutrino flux remain a viable possibility [67].

The large high altitude air shower observatory (LHAASO) [79] is a general purpose, continuously operating air shower cosmic-ray and γ-ray detector located in southwest China, which completed its construction in 2021. It mainly consists of the KM2A (kilometer square array), WCDA (water Cherenkov detector array), and WFCTA (wide field of view Cherenkov telescope array). Together, it is sensitive to the γ-ray sky from 100 GeV to 1 PeV, and has for the first time detected PeV γ rays from astrophysical sources [16,17].

In this Letter, we utilize the data from partially completed KM2A to search for signatures of DM decays.

KM2A data analysis.—KM2A is a ground-based full-duty extensive air shower (EAS) array dedicated to VHE γ-ray astronomy above 10 TeV. It has an excellent γ/hadron separation capability by using both electromagnetic particle detectors (EDs) and underground muon detectors (MDs). The EDs are plastic scintillation detectors and the MDs are water Cherenkov detectors with 2.5 m soil overburden [80]. With a large field of view, ~2 sr, KM2A covers about 60% of the sky daily [81,82].

In this Letter, we consider data from the partially completed KM2A, including 340 days from the 1/2-KM2A (2365 out of 5216 EDs and 578 out of 1188 MDs, covering an area of 0.432 km^2), from December 27, 2019 to November 30, 2020, and 230 days from the 3/4-KM2A (3978 out of 4901 EDs and 917 out of 1188 MDs, covering an area of 0.727 km^2), from December 1, 2020 to July 19, 2021. We employ the same data quality cuts, event selection, and detector simulation as in Ref. [82] for both 1/2-KM2A and 3/4-KM2A. The angular and energy resolution of the two datasets are similar, with the latter being slightly better. At 100 TeV, the angular and energy resolutions are about 0.3° and 20% [82], respectively.

The field of view of LHAASO covers the celestial northern sky (Fig. 4 in Ref. [81]). Given that the DM signal is expected to be higher with smaller galactocentric radius, and to reduce the potential diffuse astrophysical emission from the northern Fermi bubble and the Galactic plane, we consider one fiducial search region of interest (ROI), labeled as ROI_0, around $15° \leq b \leq 45°$ and $30° \leq \ell \leq 60°$. We also consider four control regions (labeled $ROI_1 - ROI_4$) away from ROI_0 for the purpose of constraining the isotropic cosmic-ray background. These regions are selected to avoid the Fermi bubbles and the Galactic plane as well.

TABLE I. Residual events after γ/hadron separation in the search (ROI_0) and control ($ROI_1 - ROI_4$) regions with an observations of 340 days with 1/2-KM2A and 230 days with 3/4-KM2A.

Energy bin $[\log_{10}(E/\mathrm{GeV})]$	N_{ROI_0}	N_{ROI_1}	N_{ROI_2}	N_{ROI_3}	N_{ROI_4}
5.0–5.2	1209	1210	1112	1160	1157
5.2–5.4	150	147	148	150	153
5.4–5.6	51	58	51	41	43
5.6–5.8	15	13	14	6	9
5.8–6.0	7	7	2	1	7
6.0–6.2	1	0	3	1	2

Importantly, we also require $ROI_1 - ROI_4$ to have the same declination and angular size (0.274 sr) as ROI_0. This ensures that all the ROIs have the same detector responses, eliminating potential systematics in the declination dependence of the detector response. Following these criteria, $ROI_1 - ROI_4$ are chosen by shifting ROI_0 along the RA direction by 90°, 135°, 240°, and 285°, respectively. The exposure time for ROI_0 to ROI_4 are 523, 510, 523, 527, and 529 days, respectively. Due to being shifted to larger galactocentric radii, the expected DM γ-ray fluxes from $ROI_1 - ROI_4$ are a factor of a few smaller than the one from ROI_0. For more details see Supplemental Material I [83].

We partition the data from 10^5 to $10^{6.2}$ GeV with 6 energy bins in logarithmic space, which are wider than the energy resolution of the detector [82]. The γ/hadron separation is then applied by considering the ratio of the detected muons and electrons [see Eq. (7) in Ref. [82]]. To further reduce the background, we adopt a more stringent γ/hadron cut parameter than the one in point-source analyses [82]. In this analysis, the γ-ray survival rate is lowered to be at least 50% of the injected gamma-ray events in detector simulation, with the cosmic-ray survival rate further lowered down to 1.86×10^{-6} around 1 PeV in the observed data (see Supplemental Material II for details and validation of the cut [83]). Even with such a strong cut, we still expect that most of the residual events are misidentified cosmic-ray events. Table I shows the events after γ/hadron separation.

The detector responses of the ROIs are obtained by tracking the ROIs through the sky and comparing with detector simulations. To handle the large ROIs and their potential nonuniform exposure, the exposure of each ROI is obtained by tracking 67 subpixels [each $\simeq(3.7\ \mathrm{deg})^2$] within each ROI and then combined. We note that even though we expect the detector responses are the same for each ROI, their responses are computed separately to take into account differences in lifetime and pointing efficiencies. The detector performance of 1/2-KM2A has been thoroughly validated with a precise measurement of the Crab Nebula [17,82,84]. Details are presented in Ref. [82], and in Supplemental Material III [83]. For 3/4-KM2A, we use the same data selection cuts, reconstruction series, and γ/hadron separation parameters as those in 1/2-KM2A. Our results are subject to the same systematic uncertainties as discussed in Ref. [82], which is estimated to be about 7% for the flux inference and mainly comes from the variation of event rate during the operational period due to seasonal and daily changes. Furthermore, to assess the systematic uncertainties due to the γ/hadron separation procedure, we find that the flux would change by about 20% if the cut condition were changed to a 30% γ-ray survival rate. The inferred DM decay rate results are thus also subject to these uncertainties.

Decaying dark matter formalism.—DM decaying into various standard model states could give rise to a diffuse flux of VHE γ rays. In the PeV energy range, the dominant γ-ray components are the prompt component generated directly from Galactic DM decays as well as the secondary component from inverse Compton (IC) scattering of electrons and positrons produced by DM particles [56,85,86]. Other contributions, such as bremsstrahlung and synchrotron radiation, are either subdominant or contribute at much lower energies. Moreover, due to the cosmic γ-ray attenuation and the related electromagnetic cascade processes, extragalactic DM decays are relevant only at energies smaller than $\sim 10^4$ GeV [87]. Thus, neglecting these contributions is conservative, and does not impact our results.

The prompt γ-ray intensity (flux per solid angle) due to DM decay from a certain Galactic latitude (b) and longitude (ℓ) is given by

$$\frac{dI_\gamma^{\rm prompt}}{dE_\gamma} = \frac{1}{4\pi m_{\rm DM}\tau_{\rm DM}}\frac{dN_\gamma}{dE_\gamma}D(E_\gamma, b, \ell), \qquad (1)$$

where $m_{\rm DM}$ and $\tau_{\rm DM}$ are, respectively, the mass and the lifetime of DM particles, dN_γ/dE_γ is the photon energy spectrum per DM decay, and $D(E_\gamma, b, \ell)$ is the so-called D factor. The photon energy spectrum is computed by using the `HDMSpectra` package [88], which includes the electroweak radiative corrections. The D factor is given by the integral of the DM halo density profile ρ_h over the line of sight s, including the effect of Galactic γ-ray attenuation,

$$D(E_\gamma, b, \ell) = \int_0^\infty ds\, \rho_h[r(s, b, \ell)] e^{-\tau_{\gamma\gamma}(E_\gamma, \vec{x})}, \qquad (2)$$

where $\tau_{\gamma\gamma}$ is the total optical depth due to pair production ($\gamma\gamma \to e^+e^-$) with background photons [56]. The photon targets are the cosmic microwave background (CMB), Galactic starlight (SL), and infrared (IR) radiation. The SL + IR background is extracted from the `GALPROPv54` code [89] (see also Ref. [90]). While the CMB photons are homogeneous, the SL + IR radiation depends on the position $\vec{x}$ in the Galaxy, which is expressed in terms of (s, b, ℓ). In particular, SL + IR dominates over CMB near the Galactic center and in the Galactic plane. Nevertheless, the angular dependence of the D factor stems mainly from the DM halo density profile, for which we consider the commonly adopted Navarro-Frenk-White (NFW) distribution [91]

$$\rho_h(r) = \frac{\rho_s}{(r/r_s)(1 + r/r_s)^2}, \qquad (3)$$

which is a function of the galactocentric radial coordinate

$$r = \sqrt{s^2 + R_\odot^2 - 2sR_\odot \cos b \cos \ell}, \qquad (4)$$

with $R_\odot = 8.3$ kpc being the Sun position. At the scale radius $r_s = 20$ kpc we take $\rho_s = 0.33$ GeV/cm^3, which yields a local DM density $\rho_\odot \simeq 0.4$ GeV cm^{-3} [92–94]. The local DM density is found to be generally around 0.3–0.6 GeV/cm^3 [95] and our DM decay results scale linearly with it. In the energy range considered, the averaged energy-dependent D factor in Eq. (2) in the search region (ROI$_0$) is larger by a factor ranging from 1.6 to 2.3 than those in the control regions (ROI$_1$ − ROI$_4$). This ensures a higher DM intensity in ROI$_0$ with respect to the other selected regions. Moreover, the DM γ-ray flux depends only slightly on the choice of the density profile for the extended DM Galactic halo and our results are robust against density profile choices, see Supplemental Material IV [83].

The secondary Galactic IC component is computed by solving the stationary diffusion-loss equation for the electrons and positrons injected in the Galaxy by DM decays. At high energies, however, the electron-positron distribution is completely dictated by the energy losses [56]. Hence, by neglecting the marginal effect of diffusion, the galactic IC component takes the following expression [56,85]:

$$\frac{dI_\gamma^{\rm IC}}{dE_\gamma} = \frac{1}{2\pi E_\gamma m_{\rm DM}\tau_{\rm DM}} \int_0^\infty ds\, \rho_h(r) e^{-\tau_{\gamma\gamma}(E_\gamma, \vec{x})} \times \int_{E_\gamma}^{\frac{m_{\rm DM}}{2}} dE_e \frac{P_{\rm IC}(E_\gamma, E_e, \vec{x})}{b(E_e, \vec{x})} \int_{E_e}^{\frac{m_{\rm DM}}{2}} dE'_e \frac{dN_e}{dE'_e}. \qquad (5)$$

Here, $P_{\rm IC}$ is the IC radiated power, $b(E_e, \vec{x})$ is the energy loss coefficient comprising IC and synchrotron processes, and dN_e/dE'_e is the injected electron spectrum computed with `HDMSpectra`. For the synchrotron energy losses we adopt the regular Galactic magnetic field model with a local

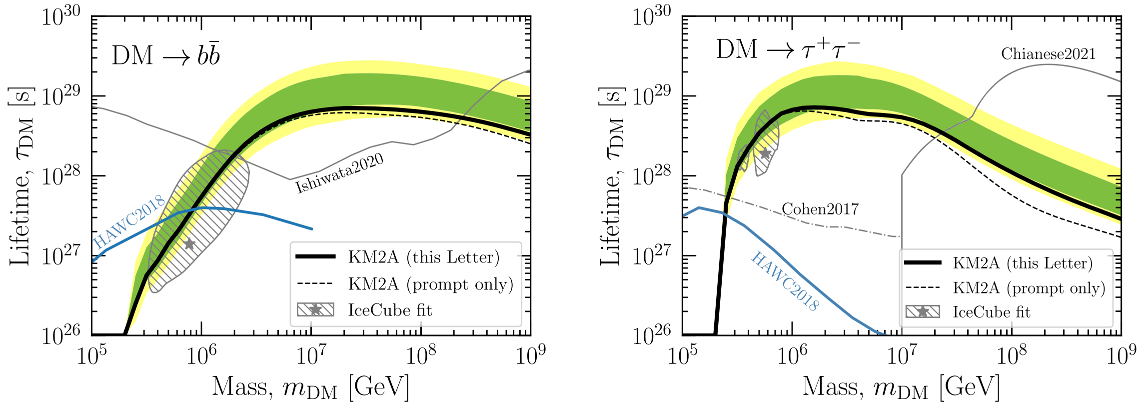

FIG. 1. 95% one-sided lower limits on DM lifetime obtained with the profile likelihood analysis (thick black lines), for DM decaying into b quarks (left) or τ leptons (right). The black dashed line shows the limit obtained if we only consider prompt DM contribution. The green and yellow bands correspond to the expected 68% and 95% limit ranges from Monte Carlo simulations with the background-only hypothesis. Previous limits [59,69,76] and those from HAWC [11] are shown with gray and blue lines. The hatched regions show the 1σ DM parameter space favored by IceCube high-energy neutrino flux [67].

strength of 4.78 μG as reported in Ref. [96]. For more details on the DM signal computation and its uncertainties, see Supplemental Material IV [83].

Likelihood analysis.—We perform a joint-likelihood analysis on the ROIs that takes into account the DM angular distribution. The likelihood function for the kth ROI is given by

$$\ln \mathcal{L}_k(\tau_{\rm DM}, b) = \sum_i N_k^i \ln n_k^i - n_k^i, \tag{6}$$

where N_k^i is the number of observed events in each energy bin, i, and n_k^i is the modeled number of events, given by

$$n_k^i(\tau_{\rm DM}, b) = (b^i + s_k^i(\tau_{\rm DM}))\mathcal{E}_k^i \Delta\Omega, \tag{7}$$

where b^i is the background model, $s_k^i(\tau_{\rm DM})$ is the total integrated DM intensity for the specific ROI,

$$s_k^i(\tau_{\rm DM}) = \frac{1}{\Delta\Omega}\int d\Omega dE_\gamma \left(\frac{dI_\gamma^{\rm prompt}}{dE_\gamma} + \frac{dI_\gamma^{\rm IC}}{dE_\gamma}\right), \tag{8}$$

$\mathcal{E}_k^i$ is the detector exposure on the ROI, and $\Delta\Omega$ is the solid angle of the ROIs.

Importantly, the DM intensity is different in different ROIs due to the different D factor and secondary contributions, while all ROIs have the same underlying background model (b^i) due to the isotropic cosmic-ray background distribution. This breaks the signal-background degeneracy between different ROIs, and thus $\mathrm{ROI}_1 - \mathrm{ROI}_4$ are included to constrain the background contribution. The background is expected to be isotropic, as the intrinsic cosmic-ray anisotropy is only ~0.1% [97,98], much smaller than the statistical uncertainties. We consider the joint-likelihood for all 5 ROIs: $\ln \mathcal{L}(\tau_{\rm DM}, \hat{b}) = \sum_{k=0}^4 \ln \mathcal{L}_k$, with the "hat" signaling that the background b^i has been treated as a nuisance parameter and fitted over to maximize the likelihood [99]. For the background model, b^i, we conservatively assume complete ignorance of their values in each energy bin, and thus they can take any non-negative values during the fit.

We search for the presence of a DM signal by scanning through the DM mass from 10^5 to 10^9 GeV for each decay channel, assuming a 100% branching fraction. We find no significant detection of DM signals, which would correspond to a peak in the likelihood function against $\tau_{\rm DM}$. Therefore, we obtain the one-sided 95% lower limit on the DM decay lifetime, $\tau_{\rm DM,95}$, for each DM mass and decay channel by finding $-2\ln[\mathcal{L}(\tau_{\rm DM,95})/\hat{\mathcal{L}}] = 2.71$ [100], where $\hat{\mathcal{L}}$ is the best-fit likelihood with respect to both $\tau_{\rm DM}$ and b.

Results.—Figure 1 shows the constraints for the DM → $b\bar{b}$ and DM → $\tau^+\tau^-$ channels obtained in this Letter (thick black lines). Other decay channels are discussed in Supplemental Material V [83]. To validate our results, we perform the same joint-likelihood analysis with mock data for the ROIs using the best-fit null-hypothesis ($\tau_{\rm DM} \to \infty$) background model and assuming a Poisson probability distribution. The 68% and 95% limit ranges from such Monte Carlo simulations are shown in Fig. 1. We find that the actual constraints are within the 95% expected range, but are close to the bottom range. This is caused by a small and statistically insignificant event excess in ROI_0 (The highest local significance found is about 1.4σ for the $\tau^+\tau^-$ channel at ~8 PeV.). The agreement with the Monte Carlo simulation also validates the common background hypothesis for the ROIs. This implies that potential anisotropic astrophysical components in the ROIs, such as diffuse emission and point sources, are subdominant. In Fig. 1 we also show the limits obtained considering only the prompt contribution to highlight the robustness of our constraints with respect to potential uncertainties in the secondary components.

For comparison, we also show the best previous limits on DM lifetime obtained with γ rays for both channels [59,69,76], including those from HAWC [11]. Hence, the present analysis leads to a significant improvement in the DM constraints. For the $b\bar{b}$ channel, our results are about 5 times better than [69] around 10 PeV, while for the $\tau^+\tau^-$ channel, they are more than 10 times better than [59] at 10 PeV. For DM masses higher than $\mathcal{O}(10^8\ \text{GeV})$, our constraints are in general weaker than those obtained with KASCADE, etc. [76]. Recently, new DM constraints [73,74] were obtained by considering the Tibet-ASγ data along the Galactic plane [18]; our constraints are generally stronger by about one order of magnitude than their model-independent limits. We emphasize that we do not consider any potential astrophysical contributions in the ROIs. Doing so will improve our constraints, but makes our results dependent on the astrophysical models.

Our limits are subject to overall systematic uncertainties, estimated to be 21%, which is a quadrature sum of uncertainties from the detector response (~7%) and γ/hadron separation procedure (~20%), and mentioned above. In addition, even with the most conservative DM density profile assumption, our limit only weakens by about 5%. These uncertainties would not affect physical interpretations of our results, as evident from Fig. 1.

In addition, even with the most conservative DM density profile assumption, our limit only weakens by about 5%. These uncertainties would not affect physical interpretations of our results, as evident from Fig. 1.

DM decays can also produce high-energy neutrinos that can be searched for with neutrino telescopes [53,54,57,62,65–68,72,75,77,78]. Our constraints are generally more stringent than those obtained with IceCube data (e.g., in Refs. [67,77]), except in neutrino channels. These searches are therefore highly complementary. See Supplemental Material VI for a comparison with the latest IceCube results [77]. Remarkably, our results highly constrain the hypothesis of decaying DM as a source of high-energy neutrinos. The limits reported in Fig. 1 disfavor a large portion of the 68% C.L. DM parameter space (hatched regions) and the best-fit scenario (black stars) inferred with the latest IceCube data [67]. We note that the DM interpretation of the IceCube data is not significant ($< 2\sigma$), and the IceCube data is still compatible with an isotropic spatial distribution.

Conclusions and outlook.—In this Letter, using 340 days of 1/2-KM2A and 230 days of 3/4-KM2A data, we obtain some of the strongest γ-ray limits on heavy decaying DM particles. This analysis shows that, even with just partial KM2A data, LHAASO already offers unprecedented sensitivity in DM indirect-detection searches, with an immediate impact on the DM interpretation of IceCube high-energy neutrino events.

This analysis uses a data-driven method to estimate the residual cosmic-ray background through the ROIs, which allows us to obtain strong yet robust constraints on the DM lifetime. In the future, with the completion of the full KM2A array, considering more sky data and longer collection time, the effective exposure can be enhanced dramatically. Considering any underlying astrophysical components would also reduce the allowed DM contribution. Furthermore, with the full LHAASO detectors (KM2A + WCDA + WFCTA), the γ/hadron separation power is expected to be further improved, with the energy range extended. Together, we expect the DM sensitivity will be significantly improved, offering new possibilities for a potential detection of DM.

The authors would like to thank all staff members who work at the LHAASO site above 4400 meters above sea level year-round to maintain the detector and keep the electrical power supply and other components of the experiment operating smoothly. We are grateful for Y. H. Yu, who cross checked the KM2A data processing. We thank Carsten Rott for helpful comments. We thank the referees for constructive comments. This work is supported in China by the National Key R&D program of China under Grants No. 2018YFA0404201, No. 2018YFA0404202, No. 2018YFA0404203, and No. 2018YFA0404204, by the NSFC under Grants No. U1931112, No. U1931201, No. 12022502, No. 11905227, No. U1831208, No. 11635011, No. 11761141001, No. 11905240, No. 11675204, No. 11475190, No. U2031105, and No. U1831129, and in Thailand by grant RTA6280002 from Thailand Science Research and Innovation. Chengdu Management Committee of Tianfu New Area provided financial support for research with LHAASO data. M. C., D. F. G. F., and G. M. acknowledge support from the research Grant No. 2017W4HA7S “NAT-NET: Ministero dell’Università e della Ricerca” under the program PRIN 2017 funded by the Italian Ministero dell’Università e della Ricerca (MUR) and from the research project TAsP (Instituto Nazionale di Fisica Nucleare) funded by the Istituto Nazionale di Fisica Nucleare (INFN). The work of D. F. G. F. is partially supported by the Villum Fonden under Project No. 29388. This project has received funding from the European Union’s Horizon 2020 research and innovation program under the Marie Sklodowska-Curie grant agreement No. 847523 “INTERACTIONS.” K. C. Y. N. acknowledges support by the Croucher Foundation. The work of S. A. was supported by JSPS/MEXT KAKENHI Grants No. JP17H04836, No. JP20H05850, and No. JP20 H05861.

*lizhe@ihep.ac.cn
†chianese@na.infn.it
‡kcyng@cuhk.edu.hk
§chensz@ihep.ac.cn

[1] Felix Kahlhoefer, Review of LHC dark matter searches, Int. J. Mod. Phys. A **32**, 1730006 (2017).
[2] Marc Schumann, Direct detection of WIMP dark matter: Concepts and status, J. Phys. G **46**, 103003 (2019).
[3] Carlos Pérez de los Heros, Status, challenges and directions in indirect dark matter searches, Symmetry **12**, 1648 (2020).
[4] Gianfranco Bertone and Tim M. P. Tait, A new era in the search for dark matter, Nature (London) **562**, 51 (2018).
[5] R. Alves Batista *et al.*, EuCAPT white paper: Opportunities and challenges for theoretical astroparticle physics in the next decade, arXiv:2110.10074.
[6] M. Ackermann *et al.* (Fermi-LAT Collaboration), Constraints on the galactic halo dark matter from fermi-LAT diffuse measurements, Astrophys. J. **761**, 91 (2012).
[7] M. Ackermann *et al.* (Fermi-LAT Collaboration), Searching for Dark Matter Annihilation from Milky Way Dwarf Spheroidal Galaxies with Six Years of Fermi Large Area Telescope Data, Phys. Rev. Lett. **115**, 231301 (2015).
[8] H. Abdalla *et al.* (H.E.S.S. Collaboration), H.E.S.S. Limits on Linelike Dark Matter Signatures in the 100 GeV to 2 TeV Energy Range Close to the Galactic Center, Phys. Rev. Lett. **117**, 151302 (2016).
[9] A. Albert *et al.* (Fermi-LAT, DES Collaborations), Searching for dark matter annihilation in recently discovered milky way satellites with fermi-LAT, Astrophys. J. **834**, 110 (2017).
[10] S. Archambault *et al.* (VERITAS Collaboration), Dark matter constraints from a joint analysis of dwarf spheroidal galaxy observations with VERITAS, Phys. Rev. D **95**, 082001 (2017).
[11] A. U. Abeysekara *et al.* (HAWC Collaboration), A search for dark matter in the galactic halo with HAWC, J. Cosmol. Astropart. Phys. 02 (2018) 049.
[12] V. A. Acciari *et al.* (MAGIC Collaboration), A search for dark matter in Triangulum II with the MAGIC telescopes, Phys. Dark Universe **28**, 100529 (2020).
[13] A. Abramowski *et al.* (H.E.S.S. Collaboration), Acceleration of petaelectronvolt protons in the galactic centre, Nature (London) **531**, 476 (2016).
[14] A. U. Abeysekara *et al.* (HAWC Collaboration), Multiple Galactic Sources with Emission Above 56 TeV Detected by HAWC, Phys. Rev. Lett. **124**, 021102 (2020).
[15] D. D. Dzhappuev *et al.* (Carpet–3 Collaboration), Observation of photons above 300 TeV associated with a high-energy neutrino from the Cygnus Cocoon region, Astrophys. J. Lett. **916**, L22 (2021).
[16] Zhen Cao *et al.* (LHAASO Collaboration), Ultrahigh-energy photons up to 1.4 petaelectronvolts from 12 γ-ray Galactic sources, Nature (London) **594**, 33 (2021).
[17] Zhen Cao *et al.* (LHAASO Collaboration), PeV gamma-ray emission from the Crab Nebula, Science **373**, 1336 (2021).
[18] M. Amenomori *et al.* (Tibet ASgamma Collaboration), First Detection of sub-PeV Diffuse Gamma Rays from the Galactic Disk: Evidence for Ubiquitous Galactic Cosmic Rays beyond PeV Energies, Phys. Rev. Lett. **126**, 141101 (2021).
[19] M. C. Chantell, C. E. Covault, J. W. Cronin, B. E. Fick, L. F. Fortson *et al.* (CASA-MIA Collaboration), Limits on the Isotropic Diffuse Flux of Ultrahigh-Energy Gamma Radiation, Phys. Rev. Lett. **79**, 1805 (1997).
[20] W. D. Apel *et al.* (KASCADE Grande Collaboration), KASCADE-grande limits on the isotropic diffuse gamma-ray flux between 100 TeV and 1 EeV, Astrophys. J. **848**, 1 (2017).
[21] J. Patrick Harding (HAWC Collaboration), Constraints on the diffuse gamma-ray background with HAWC, Proc. Sci., ICRC2019 (**2020**) 691 [arXiv:1908.11485].
[22] Kim Griest and Marc Kamionkowski, Unitarity Limits on the Mass and Radius of Dark Matter Particles, Phys. Rev. Lett. **64**, 615 (1990).
[23] Daniel J. H. Chung, Edward W. Kolb, and Antonio Riotto, Superheavy dark matter, Phys. Rev. D **59**, 023501 (1998).
[24] Karim Benakli, John R. Ellis, and Dimitri V. Nanopoulos, Natural candidates for superheavy dark matter in string and M theory, Phys. Rev. D **59**, 047301 (1999).
[25] Edward W. Kolb, Daniel J. H. Chung, and Antonio Riotto, WIMPzillas! AIP Conf. Proc. **484**, 91 (1999).
[26] Alon E. Faraggi and Maxim Pospelov, Selfinteracting dark matter from the hidden heterotic string sector, Astropart. Phys. **16**, 451 (2002).
[27] Kimberly K. Boddy, Jonathan L. Feng, Manoj Kaplinghat, and Tim M. P. Tait, Self-interacting dark matter from a non-Abelian hidden sector, Phys. Rev. D **89**, 115017 (2014).
[28] Lindsay Forestell, David E. Morrissey, and Kris Sigurdson, Non-Abelian dark forces and the relic densities of dark glueballs, Phys. Rev. D **95**, 015032 (2017).
[29] James Halverson, Brent D. Nelson, and Fabian Ruehle, String theory and the dark glueball problem, Phys. Rev. D **95**, 043527 (2017).
[30] Heinz Pagels and Joel R. Primack, Supersymmetry, Cosmology and New TeV Physics, Phys. Rev. Lett. **48**, 223 (1982).
[31] Frank Daniel Steffen, Gravitino dark matter and cosmological constraints, J. Cosmol. Astropart. Phys. 09 (2006) 001.
[32] Koji Ishiwata, Shigeki Matsumoto, and Takeo Moroi, High energy cosmic rays from the decay of gravitino dark matter, Phys. Rev. D **78**, 063505 (2008).
[33] Mathias Garny, McCullen Sandora, and Martin S. Sloth, Planckian Interacting Massive Particles as Dark Matter, Phys. Rev. Lett. **116**, 101302 (2016).
[34] M. Re Fiorentin, V. Niro, and N. Fornengo, A consistent model for leptogenesis, dark matter and the IceCube signal, J. High Energy Phys. 11 (2016) 022.
[35] Marco Chianese and Alexander Merle, A consistent theory of decaying dark matter connecting IceCube to the Sesame Street, J. Cosmol. Astropart. Phys. 04 (2017) 017.
[36] Edward W. Kolb and Andrew J. Long, Superheavy dark matter through Higgs portal operators, Phys. Rev. D **96**, 103540 (2017).
[37] Tetsutaro Higaki, Ryuichiro Kitano, and Ryosuke Sato, Neutrinoful universe, J. High Energy Phys. 07 (2014) 044.

[38] P. S. Bhupal Dev, D. Kazanas, R. N. Mohapatra, V. L. Teplitz, and Yongchao Zhang, Heavy right-handed neutrino dark matter and PeV neutrinos at IceCube, J. Cosmol. Astropart. Phys. 08 (2016) 034.

[39] Pasquale Di Bari, Patrick Otto Ludl, and Sergio Palomares-Ruiz, Unifying leptogenesis, dark matter and high-energy neutrinos with right-handed neutrino mixing via Higgs portal, J. Cosmol. Astropart. Phys. 11 (2016) 044.

[40] Roberto Contino, Andrea Mitridate, Alessandro Podo, and Michele Redi, Gluequark dark matter, J. High Energy Phys. 02 (2019) 187.

[41] Eugeny Babichev, Dmitry Gorbunov, and Sabir Ramazanov, New mechanism of producing superheavy dark matter, Phys. Lett. B **794**, 69 (2019).

[42] Hyungjin Kim and Eric Kuflik, Superheavy Thermal Dark Matter, Phys. Rev. Lett. **123**, 191801 (2019).

[43] Emilian Dudas, Lucien Heurtier, Yann Mambrini, Keith A. Olive, and Mathias Pierre, Model of metastable EeV dark matter, Phys. Rev. D **101**, 115029 (2020).

[44] Eric David Kramer, Eric Kuflik, Noam Levi, Nadav Joseph Outmezguine, and Joshua T. Ruderman, Heavy Thermal Dark Matter from a New Collision Mechanism, Phys. Rev. Lett. **126**, 081802 (2021).

[45] Thomas Hambye, Matteo Lucca, and Laurent Vanderheyden, Dark matter as a heavy thermal hot relic, Phys. Lett. B **807**, 135553 (2020).

[46] Marcos A. G. Garcia, Yann Mambrini, Keith A. Olive, and Sarunas Verner, Case for decaying spin-$3/2$ dark matter, Phys. Rev. D **102**, 083533 (2020).

[47] Brian Feldstein, Alexander Kusenko, Shigeki Matsumoto, and Tsutomu T. Yanagida, Neutrinos at IceCube from heavy decaying dark matter, Phys. Rev. D **88**, 015004 (2013).

[48] Arman Esmaili and Pasquale Dario Serpico, Are IceCube neutrinos unveiling PeV-scale decaying dark matter?, J. Cosmol. Astropart. Phys. 11 (2013) 054.

[49] Marco Chianese, Gennaro Miele, Stefano Morisi, and Edoardo Vitagliano, Low energy IceCube data and a possible dark matter related excess, Phys. Lett. B **757**, 251 (2016).

[50] M. G. Aartsen *et al.* (IceCube Collaboration), Evidence for high-energy extraterrestrial neutrinos at the IceCube detector, Science **342**, 1242856 (2013).

[51] M. G. Aartsen *et al.* (IceCube Collaboration), Observation of High-Energy Astrophysical Neutrinos in Three Years of IceCube Data, Phys. Rev. Lett. **113**, 101101 (2014).

[52] R. Abbasi *et al.* (IceCube Collaboration), The IceCube high-energy starting event sample: Description and flux characterization with 7.5 years of data, Phys. Rev. D **104**, 022002 (2021).

[53] Arman Esmaili, Alejandro Ibarra, and Orlando L. G. Peres, Probing the stability of superheavy dark matter particles with high-energy neutrinos, J. Cosmol. Astropart. Phys. 11 (2012) 034.

[54] Kohta Murase and John F. Beacom, Constraining very heavy dark matter using diffuse backgrounds of neutrinos and cascaded gamma rays, J. Cosmol. Astropart. Phys. 10 (2012) 043.

[55] Arman Esmaili, Sin Kyu Kang, and Pasquale Dario Serpico, IceCube events and decaying dark matter: Hints and constraints, J. Cosmol. Astropart. Phys. 12 (2014) 054.

[56] Arman Esmaili and Pasquale Dario Serpico, Gamma-ray bounds from EAS detectors and heavy decaying dark matter constraints, J. Cosmol. Astropart. Phys. 10 (2015) 014.

[57] Kohta Murase, Ranjan Laha, Shin'ichiro Ando, and Markus Ahlers, Testing the Dark Matter Scenario for PeV Neutrinos Observed in IceCube, Phys. Rev. Lett. **115**, 071301 (2015).

[58] M. Chianese, G. Miele, and S. Morisi, Dark matter interpretation of low energy IceCube MESE excess, J. Cosmol. Astropart. Phys. 01 (2017) 007.

[59] Timothy Cohen, Kohta Murase, Nicholas L. Rodd, Benjamin R. Safdi, and Yotam Soreq, γ -ray Constraints on Decaying Dark Matter and Implications for IceCube, Phys. Rev. Lett. **119**, 021102 (2017).

[60] Atri Bhattacharya, Arman Esmaili, Sergio Palomares-Ruiz, and Ina Sarcevic, Probing decaying heavy dark matter with the 4-year IceCube HESE data, J. Cosmol. Astropart. Phys. 07 (2017) 027.

[61] Marco Chianese, Gennaro Miele, and Stefano Morisi, Interpreting IceCube 6-year HESE data as an evidence for hundred TeV decaying dark matter, Phys. Lett. B **773**, 591 (2017).

[62] M. G. Aartsen *et al.* (IceCube Collaboration), Search for neutrinos from decaying dark matter with IceCube, Eur. Phys. J. C **78**, 831 (2018).

[63] M. Kachelriess, O. E. Kalashev, and M. Yu. Kuznetsov, Heavy decaying dark matter and IceCube high energy neutrinos, Phys. Rev. D **98**, 083016 (2018).

[64] Carlos Blanco and Dan Hooper, Constraints on decaying dark matter from the isotropic gamma-ray background, J. Cosmol. Astropart. Phys. 03 (2019) 019.

[65] Atri Bhattacharya, Arman Esmaili, Sergio Palomares-Ruiz, and Ina Sarcevic, Update on decaying and annihilating heavy dark matter with the 6-year IceCube HESE data, J. Cosmol. Astropart. Phys. 05 (2019) 051.

[66] Carlos A. Argüelles and Hrvoje Dujmovic (IceCube Collaboration), Searches for connections between dark matter and neutrinos with the IceCube high-energy starting event sample, Proc. Sci., ICRC2019 (**2020**) 839 [arXiv:1907.11193].

[67] Marco Chianese, Damiano F. G. Fiorillo, Gennaro Miele, Stefano Morisi, and Ofelia Pisanti, Decaying dark matter at IceCube and its signature on High Energy gamma experiments, J. Cosmol. Astropart. Phys. 11 (2019) 046.

[68] Ariane Dekker, Marco Chianese, and Shin'ichiro Ando, Probing dark matter signals in neutrino telescopes through angular power spectrum, J. Cosmol. Astropart. Phys. 09 (2020) 007.

[69] Koji Ishiwata, Oscar Macias, Shin'ichiro Ando, and Makoto Arimoto, Probing heavy dark matter decays with multi-messenger astrophysical data, J. Cosmol. Astropart. Phys. 01 (2020) 003.

[70] Aion Viana, Harm Schoorlemmer, Andrea Albert, Vitor de Souza, J. Patrick Harding, and Jim Hinton, Searching for dark matter in the galactic halo with a wide field of view TeV gamma-ray observatory in the southern hemisphere, J. Cosmol. Astropart. Phys. 12 (2019) 061.

[71] Andrii Neronov and Dmitri Semikoz, LHAASO telescope sensitivity to diffuse gamma-ray signals from the galaxy, Phys. Rev. D **102**, 043025 (2020).

[72] Kenny C. Y. Ng *et al.*, Sensitivities of KM3NeT on decaying dark matter, arXiv:2007.03692.

[73] Arman Esmaili and Pasquale D. Serpico, First implications of Tibet ASγ data for heavy dark matter, Phys. Rev. D **104**, L021301 (2021).

[74] Tarak Nath Maity, Akash Kumar Saha, Abhishek Dubey, and Ranjan Laha, A search for dark matter using sub-PeV γ-rays observed by Tibet AS$_\gamma$, Phys. Rev. D **105**, L041301 (2022).

[75] Marco Chianese, Damiano F. G. Fiorillo, Rasmi Hajjar, Gennaro Miele, Stefano Morisi, and Ninetta Saviano, Heavy decaying dark matter at future neutrino radio telescopes, J. Cosmol. Astropart. Phys. 05 (2021) 074.

[76] Marco Chianese, Damiano F. G. Fiorillo, Rasmi Hajjar, Gennaro Miele, and Ninetta Saviano, Constraints on heavy decaying dark matter with current gamma-ray measurements, J. Cosmol. Astropart. Phys. 11 (2021) 035.

[77] R. Abbasi *et al.* (IceCube Collaboration), Searches for Connections between Dark Matter and High-Energy Neutrinos with IceCube, arXiv:2205.12950.

[78] R. Abbasi *et al.* (IceCube Collaboration), Search for Dark Matter from the Galactic Halo with the IceCube Neutrino Observatory, arXiv:1101.3349.

[79] Cao Zhen *et al.* (LHAASO Collaboration), Introduction to large high altitude air shower observatory (LHAASO), Chin. Astron. Astrophys. **43**, 457 (2019).

[80] Huihai He, Design of the lhaaso detectors, Radiat. Detect. Technol. Methods **2**, 7 (2018).

[81] X. Bai *et al.*, The large high altitude air shower observatory (LHAASO) science white paper: Chapter 2 galactic gamma-ray sources, Chin. Phys. C **45**, 035002 (2022).

[82] F. Aharonian *et al.*, Observation of the Crab Nebula with LHAASO-KM2A–a performance study, Chin. Phys. C **45**, 025002 (2021).

[83] See Supplemental Material at http://link.aps.org/supplemental/10.1103/PhysRevLett.129.261103 for additional details and results.

[84] Songzhan Chen, Detector simulation of LHAASO-KM2A with Geant4, Proc. Sci., ICRC2019 (**2020**) 219.

[85] Marco Cirelli, Gennaro Corcella, Andi Hektor, Gert Hutsi, Mario Kadastik, Paolo Panci, Martti Raidal, Filippo Sala, and Alessandro Strumia, PPPC 4 DM ID: A poor particle physicist cookbook for dark matter indirect detection, J. Cosmol. Astropart. Phys. 03 (2011) 051; 10 (2012) E01.

[86] Jatan Buch, Marco Cirelli, Gaëlle Giesen, and Marco Taoso, PPPC 4 DM secondary: A poor particle Physicist Cookbook for secondary radiation from dark matter, J. Cosmol. Astropart. Phys. 09 (2015) 037.

[87] V. Berezinsky and O. Kalashev, High energy electromagnetic cascades in extragalactic space: Physics and features, Phys. Rev. D **94**, 023007 (2016).

[88] Christian W. Bauer, Nicholas L. Rodd, and Bryan R. Webber, Dark matter spectra from the electroweak to the Planck scale, J. High Energy Phys. 06 (2021) 121.

[89] https://galprop.stanford.edu/.

[90] Troy A. Porter, Gudlaugur Johannesson, and Igor V. Moskalenko, High-energy gamma rays from the milky way: Three-dimensional spatial models for the cosmic-ray and radiation field densities in the interstellar medium, Astrophys. J. **846**, 67 (2017).

[91] Julio F. Navarro, Carlos S. Frenk, and Simon D. M. White, A universal density profile from hierarchical clustering, Astrophys. J. **490**, 493 (1997).

[92] Riccardo Catena and Piero Ullio, A novel determination of the local dark matter density, J. Cosmol. Astropart. Phys. 08 (2010) 004.

[93] Fabio Iocco, Miguel Pato, and Gianfranco Bertone, Evidence for dark matter in the inner milky way, Nat. Phys. **11**, 245 (2015).

[94] Miguel Pato, Fabio Iocco, and Gianfranco Bertone, Dynamical constraints on the dark matter distribution in the milky way, J. Cosmol. Astropart. Phys. 12 (2015) 001.

[95] Pablo F. de Salas and Axel Widmark, Dark matter local density determination: Recent observations and future prospects, Rep. Prog. Phys. **84**, 104901 (2021).

[96] Andrew W. Strong, Igor V. Moskalenko, and Olaf Reimer, Diffuse continuum gamma-rays from the galaxy, Astrophys. J. **537**, 763 (2000); **541**, 1109(E) (2000).

[97] M. G. Aartsen *et al.* (IceCube Collaboration), Observation of cosmic-ray anisotropy with the IceTop air shower array, Astrophys. J. **765**, 55 (2013).

[98] A. U. Abeysekara *et al.*, Observation of anisotropy of TeV cosmic rays with two years of HAWC, Astrophys. J. **865**, 57 (2018).

[99] Wolfgang A. Rolke, Angel M. Lopez, and Jan Conrad, Limits and confidence intervals in the presence of nuisance parameters, Nucl. Instrum. Methods Phys. Res., Sect. A **551**, 493 (2005).

[100] Glen Cowan, Kyle Cranmer, Eilam Gross, and Ofer Vitells, Asymptotic formulae for likelihood-based tests of new physics, Eur. Phys. J. C **71**, 1554 (2011); **73**, 2501(E) (2013).